nature energy

PERSPECTIVE

https://doi.org/10.1038/s41560-020-00772-8

Assessment methods and performance metrics for redox flow batteries

Yanxin Yao, Jiafeng Lei, Yang Shi, Fei Ai and Yi-Chun Lu ✉

Redox flow batteries (RFBs) are a promising technology for large-scale energy storage. Rapid research developments in RFB chemistries, materials and devices have laid critical foundations for cost-effective and long-lasting RFB systems. However, the lack of consistency in testing methods and assessment metrics makes it challenging to compare reported RFBs and evaluate their potential for practical applications. Here we discuss RFB assessment methods and performance metrics in direct relation to their working principles and degradation mechanisms. We first introduce basic cell attributes and performance metrics and describe common misconceptions in testing and performance comparison. We discuss major RFB decay mechanisms and highlight bottlenecks in organic, inorganic and solid-hybrid RFBs. Testing protocols, reporting practices and comparison criteria are proposed under a general framework of symmetric and asymmetric full RFBs. These recommendations can be broadly applied to a wide range of flow battery chemistries to facilitate future benchmarking and RFB development.

The energy storage system (EES) is the bottleneck to the development of a smart/micro-grid and the widespread use of intermittent renewable power sources. Developing a high-energy, low-cost and reliable ESS will accelerate the transition from a fossil-fuel-based energy dependence to clean and renewable energy at a global scale. Redox flow batteries (RFBs) are an important EES that stores electrical energy in two redox-active species with distinct redox potentials dissolved or suspended in the electrolyte tanks (negolyte and posolyte in Fig. 1a). Electrochemical charge-transfer reactions occur on the electrode stack, which consists of a pair of porous electrodes separated by an ion-conducting membrane. The capacity of the RFB scales with available charges stored in the electrolyte tank while the current output of the RFB is determined by the rate of the electrochemical reaction on the electrode stack. This unique configuration enables design flexibility in decoupling energy and power, which is critical for large-scale and distributed energy storage[1].

State-of-the-art all-vanadium RFBs are limited by their low energy density and high vanadium cost[2], which motivated worldwide research development for new RFB materials. However, the lack of consistency in testing methods and assessment metrics makes it challenging to compare reported RFBs and evaluate their potential for practical applications. Arbitrary testing conditions and misconceptions in performance metrics prevent meaningful comparisons and further development for RFBs.

In this Perspective, we discuss assessment methods and performance metrics in direct relation to the working principles and degradation mechanisms of RFBs. We start by introducing basic cell attributes and performance metrics, along with a description of common misconceptions in testing and performance comparison. We also recommend minimal requirements for some of the key testing parameters. This is followed by discussions on major decay mechanisms in RFBs. Finally, we propose a general framework of testing protocols, reporting practices and comparison criteria.

Key cell attributes and performance metrics

We categorize most of the RFBs into all-liquid RFBs and solid-hybrid RFBs based on the nature of the redox reactions. In all-liquid RFBs, all the redox-active species involved are soluble in the electrolyte, for example, all-vanadium RFBs[2], organic RFBs[3,4], polysulfide/iodide RFBs[5] and so on. In solid-hybrid RFBs, at least one of the electrode reactions involves solid deposition/dissolution, for example, zinc-based RFBs[6–8], lithium-based RFBs[9], Mn^{2+}/MnO_2-based RFBs[10] and so on. All-liquid RFBs allow full decoupling of energy and power with high scalability; however, they often suffer from low energy density. In contrast, solid-hybrid RFBs promise high energy density at the expense of design flexibility and scalability[11].

We define basic cell attributes and performance metrics in Table 1. The electromotive force of the RFB can be evaluated from the open-circuit cell voltage ($V_{cell,OCV}$, equation (1)) at 50% state-of-charge (SOC, equation (4)) which is the ratio of charged capacity stored over theoretical capacity. Theoretical capacity of posolyte or negolyte ($Q_{t,+/-}$, equation (2)) is determined by the number of electrons transferred (n), concentration of the electrolyte (c) and the volume of the electrolyte (v). Geometric current density is the current output per membrane area (I_a, equation (3)). For solid-hybrid RFBs, the areal capacity of the solid-based reaction ($Q_{a(solid)}$, equation (5)) is the achieved reversible capacity (Q_{rev}) divided by the membrane area (A). These factors substantially affect overall RFB performance and shall be controlled and considered collectively when making comparisons.

Volumetric capacity and energy. Volumetric capacity of negolyte or posolyte ($Q_{v,+/-}$, equation (6)) evaluates the available charge capacity per unit volume of the electrolyte, which is critical in projecting the footprint of the RFB tank for large-scale applications. When reporting and comparing volumetric capacity, the electrolyte volume used for calculation (posolyte, negolyte or both) should be clearly stated to avoid biased comparisons. The volumetric cell capacity ($Q_{v,cell}$) is determined by the volumetric capacity of posolyte and negolyte ($Q_{v,+/-}$, equation (7)). The volumetric energy density of the cell ($E_{v,cell}$, equation (9)) is obtained by integrating the discharge curves of cell voltage (V_{cell}) and cell volumetric capacity ($Q_{v,cell}$). When reporting the volumetric energy density of the cell, both posolyte and negolyte volume should be included.

Electrochemical Energy and Interfaces Laboratory, Department of Mechanical and Automation Engineering, The Chinese University of Hong Kong, Hong Kong SAR, China. ✉e-mail: yichunlu@mae.cuhk.edu.hk

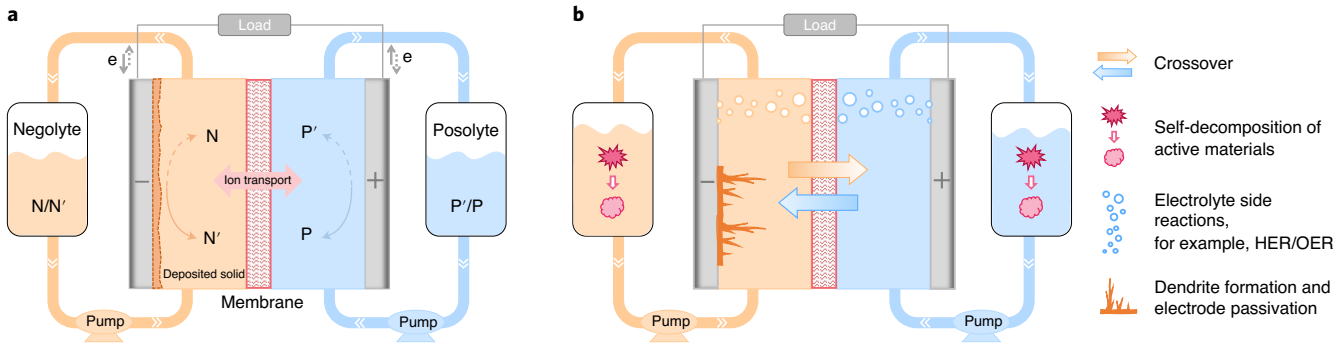

Fig. 1 | Fundamental illustrations of RFBs. a, A schematic representation of a general RFB cell. The solid and dashed curly arrows represent the charging and discharging process, respectively. N/N′, negolyte in oxidized/reduced state; P/P′, posolyte in oxidized/reduced state. **b**, Common degradation mechanisms of RFBs, including crossover, self-decomposition of active materials, electrolyte side reactions, and dendrite formation and electrode passivation.

For solid-hybrid RFBs involving solid-based reactions (for example, zinc-based RFBs), when the practically achieved solid electrode capacity is lower than the available capacity stored in the liquid phase, the volumetric capacity of the electrolyte ($Q_{v,+/-}$) becomes limited by the solid electrode capacity. That is, even if there is more capacity available in the liquid electrolyte, if solid deposition reaction cannot continue due to certain limitations (for example, dendrite, electrode passivation and so on), it becomes the limiting factor for total cell capacity. Therefore, the areal capacity of the solid reaction ($Q_{a(solid)}$) is a critical factor when evaluating solid-hybrid RFBs[6,10], and should be controlled to avoid biased comparison/conclusion.

We show an example in Fig. 2a of how the areal capacity could differ substantially in different cycling conditions even if the same membrane area and the same volumetric capacity are applied. Because of the ten times difference in the electrolyte volume, the effective areal capacities differ by ten times. Consequently, the cell cycling at the higher areal capacity would be more prone to dendrite formation/degradation owing to a harsher cycling condition. Therefore, areal capacity should be considered and controlled while studying/comparing the solid-hybrid RFBs as it largely affects the practical volumetric capacity, energy and lifetime of the solid-hybrid RFBs.

Capacity fade rate and Coulombic efficiency. Capacity fade rate is used to evaluate the cycling stability of RFBs and can be quantified against time (% per day) or cycle number (% per cycle). These are useful metrics adopted in the community and their relative importance varies based on the most critical degradation mechanism of the RFBs[12].

Coulombic efficiency (CE, equation (8)) is a useful metric for assessing the charge reversibility of each cycle[13,14]. CE loss can be contributed to by capacity-related processes and non-capacity-related processes[15]. Therefore, the direct analytical correlation between CE and capacity retention (or fade) is circumstantial. Both CE and capacity fade rate should be analysed and reported.

In general, when one side of the electrolyte possesses enough excess charge (in both oxidized and reduced states), the capacity-related CE loss mainly arises from losses of active materials at the limited side (for example, decomposition, crossover, incomplete dissolution of solid electrode and so on). The non-capacity-related CE loss mainly comes from self-discharge at the limited side due to crossover from the excess side, and electrolyte side reactions that produce no harmful products (for example, oxygen evolution reaction (OER)/hydrogen evolution reaction (HER)). Self-discharge reduces the apparent discharge capacity but not the total cell available capacity. For electrolyte side reactions that produce no harmful products, they decrease the CE but do not irreversibly destroy active materials. For instance, if there is no sufficient charged species at the excess side to support the discharge reaction at the limiting side due to parasitic electrolyte side reactions, it will decrease the apparent capacity but not the total cell available capacity as no active materials are destroyed. Quantifying and differentiating different sources of CE losses help to develop effective improvement strategies. Therefore, it is important to simultaneously report discharge/charge capacity along with CE and energy efficiency (EE, equation (10)) for comprehensive electrochemical evaluations.

In addition, capacity fade could be hidden in the electrochemical cycling test if it was not conducted under 100% SOC. For example, as shown in Fig. 2b, if the cell is cycling at 50% SOC, even if the total available capacity decays during cycling (indicated by the dashed line), the apparent discharge capacity (solid line) may stay stable for a while, giving a false impression of the cycling stability. However, 100% SOC represents a very challenging operating condition that isn't commonly used in the commercially available batteries. Therefore, measuring the concentration of the electroactive species via quantitative spectroscopic methods[16] could be used along with electrochemical characterizations at practical SOCs to evaluate the stability of the active materials given sufficient resolution of the concentration measurements.

To discuss suitable targets for practical electron concentration (volumetric capacity) and solid areal capacity, we summarize reported volumetric capacity (Fig. 2c) and areal capacity (Fig. 2d) from representative all-liquid RFBs and solid-hybrid RFBs in relation to other key performance metrics, as a function of current density obtained at flow modes.

Considering that the electron concentration/volumetric capacity of commercial all-vanadium RFBs[17] ranges from 1.0 to 2.0 e mol^{-1} (26.8–53.6 Ah l^{-1}) and that many of the reported studies achieved beyond 1.0 e mol^{-1} (26.8 Ah l^{-1}, Fig. 2c), we recommend a minimum electron concentration of 1.0 e mol^{-1} for a cycling test. To achieve high-energy-density RFBs, it is important to demonstrate stable RFB cycling with a capacity decay rate <0.01% per day (nearly 80% capacity retention after five years) and an electron concentration of 3.0 e mol^{-1} (80.4 Ah l^{-1}) or above.

The target areal capacity of solid-hybrid RFBs is directly related to rated current density and discharge time (E/P, energy-to-power ratio, in hours). Based on the product specification of a commercial zinc-bromine RFB from RedFlow (product number ZBM2), the discharge time at 45 mA cm_{geo}^{-2} is ~3.1 h, amounting to ~140 mAh cm_{geo}^{-2} areal capacity of zinc. As shown in Fig. 2d, most of the reported literature achieved reversible cycling (>20 cycles) at an areal capacity of 20 mAh cm_{geo}^{-2} or above, which is still seven times lower than the commercial zinc-bromine RFB. Given that most of the applications

Table 1 | Cell attributes and performance metrics of RFBs

	Definition	Remarks
Cell attributes		
$V_{cell,OCV}$ at 50% SOC	$V_{cell,OCV} = V_+ - V_-$ (V) (1)	The electromotive force of the RFB at 50% SOC.
Theoretical electrolyte capacity[a]	$Q_t = n \times c \times v \times F/3,600 = ncv \times 26.8$ (mAh) (2)	Theoretical capacity stored in a given volume of electrolyte.
Current density[b]	$I_a = I/A$ (mA cm^{-2}_{geo}) (3)	Current applied per membrane area.
SOC	$SOC = Q_{charge}/Q_t$ (4)	Charged capacity stored over theoretical capacity.
Solid areal capacity	$Q_{a(solid)} = Q_{rev}/A$ (mAh cm^{-2}_{geo}) (5)	Achieved reversible capacity stored per membrane area.
Performance metrics		
Volumetric capacity	$Q_{v,+/-} = \frac{Q_{discharge,+/-}}{v_{+/-}} \left(Ah\ l^{-1}_{pos./neg.}\right)$ (6) $Q_{v,cell} = \frac{Q_{discharge}}{v_+ + v_-} = \frac{Q_{v+} \times Q_{v-}}{Q_{v+} + Q_{v-}} \left(Ah\ l^{-1}_{pos.+neg.}\right)$ (7)	Discharge capacity stored per unit volume of electrolyte (posolyte, negolyte or both).
Capacity decay rate	Slope of capacity-time or capacity-cycle number plots divide by initial capacity (% per day or % per cycle)	Capacity decay in percentage over a total test duration time (% per day) or cycle number (% per cycle). Total duration or cycle number should be reported along with decay rate.
Coulombic efficiency	$CE = Q_{discharge}/Q_{charge}$ (8)	The ratio of discharge capacity over charge capacity.
Energy density[c]	$E_{v,cell} = \frac{\int dQ_{discharge} \times dV_{cell}}{v_+ + v_-} \left(Wh\ l^{-1}_{pos.+neg.}\right)$ (9)	Energy output per unit volume of total electrolyte (both posolyte and negolyte).
Energy efficiency	$EE = E_{v,cell\ discharge}/E_{v,cell\ charge}$ (10)	The ratio of discharge energy over charge energy at certain current density.
Power density	$P = (I \times V_{cell})/A$ (mW cm^{-2}_{geo}) (11)	Power output per membrane area at a certain SOC.

[a]c is concentration (mol l^{-1}), n is the number of electrons per mole, v is volume (ml) and F is the Faraday constant. [b]I is current (mA) and A is active area (cm^{-2}_{geo}, membrane area). [c]V_{cell} is the cell voltage at the corresponding current (V).

require a discharge duration (E/P) of 2–4 h, the practical target areal capacity ranges from 100 to 200 mAh cm^{-2}_{geo} at a moderate current density of 50 mA cm^{-2}_{geo}. As such, we recommend a minimum areal capacity of 20 mAh cm^{-2}_{geo} for a cycling test and a practical application target of 150 mAh cm^{-2}_{geo} and above for solid-hybrid RFBs.

Decay mechanisms and their roles in performance metrics

Understanding the dominant decay mechanisms of RFBs helps to guide and design suitable assessment methods that can directly probe the limiting processes. We categorize major degradation mechanisms of RFBs into crossover, self-decomposition of active materials, electrolyte side reactions, and dendrite formation and electrode passivation (Fig. 1b). We discuss how they affect the relative importance of time-dependent or cycle-denominated performance metrics.

Crossover. Crossover in RFBs mainly refers to transportation of redox-active species across the ion-conducting membrane leading to self-discharge, irreversible reactions, low CE and/or capacity decay. The degree of crossover can be reduced by Donnan effect and size exclusion coupling with membrane selection for both inorganic and organic RFBs[18–20]. However, perfect selectivity is challenging to achieve in practice. Crossover represents one of the most critical challenges for inorganic RFBs, including iron-based (iron–chromium)[19], manganese-based (Mn^{2+}/Mn^{3+})[21], vanadium-based[22], polysulfide-based[23], iodide-based[5,24] RFBs and so on. The amount of tolerable crossover and related CE losses depends on whether the crossover species are irreversibly destroyed and whether the side products are detrimental to the system[14,18]. For instance, the crossover capacity in RFBs with common active materials (for example, vanadium RFBs) and 'inert spectators' (for example, iron–chromium RFBs) could be recovered by rebalancing[18]. It was suggested that a CE of 97% can be tolerated when the active species can be recovered, but a high CE of more than 99.99% is required for practical applications when the crossover species are permanently destroyed[14]. As the crossover rate at different charge states could vary substantially[25], crossover measurement at various SOCs could help to evaluate how active materials crossover at various stages over long-term cycling. In addition, water and other supporting ions could also migrate across the membrane due to osmotic pressure leading to volume imbalance and pH fluctuation.

When crossover is the major degradation mechanism, time-dependent capacity decay (% per day)[26] over a total period of time (day) would be an important assessment metric as it directly correlates to time-dependent crossover processes. In the case when only oxidized or reduced species suffer from crossover (selective crossover)[27], cycle number denominated capacity decay rate (% per cycle) could be used together with the time-dependent decay rate to assess the RFB stability. Note that the concentration of active material should be considered when making these comparisons as crossover usually accelerates with active material concentration. In addition, other cell testing parameters will also affect the apparent capacity decay rate. For example, one could minimize the decay rate by increasing membrane thickness (both % per cycle and % per day), using a high current density (% per cycle) or employing a very small cell area (% per day), even when the intrinsic rate of crossover is high. Therefore, comparisons should be conducted with identical or similar testing conditions to avoid biased conclusions. In addition, H-cell type permeation measurements coupled with ultraviolet–visible spectroscopy can be used to probe crossover rate at various SOCs and concentrations[28]. However, it only serves as a supplementary analysis as no electric field is present in the H-cell measurement, which could accelerate crossover in RFBs.

Self-decomposition of active materials. Chemical decomposition of redox-active species resulting from their intrinsic instability[12,29,30] is categorized as self-decomposition. This decay mechanism is prominently observed in organic-based RFBs (quinones[4], viologens[31], aza-aromatics[30], nitroxide radicals[32] and ferrocene[33]). It has four major types: nucleophilic addition or substitution[4,34], disproportionation[35], dimerization or polymerization[28,32], and tautomerization[36]. In addition to organic RFBs, the precipitation of inorganic dissolved active materials (from disproportionation reaction[21], hydrolysis reaction[37], irreversible chemical reaction[38] and so on)

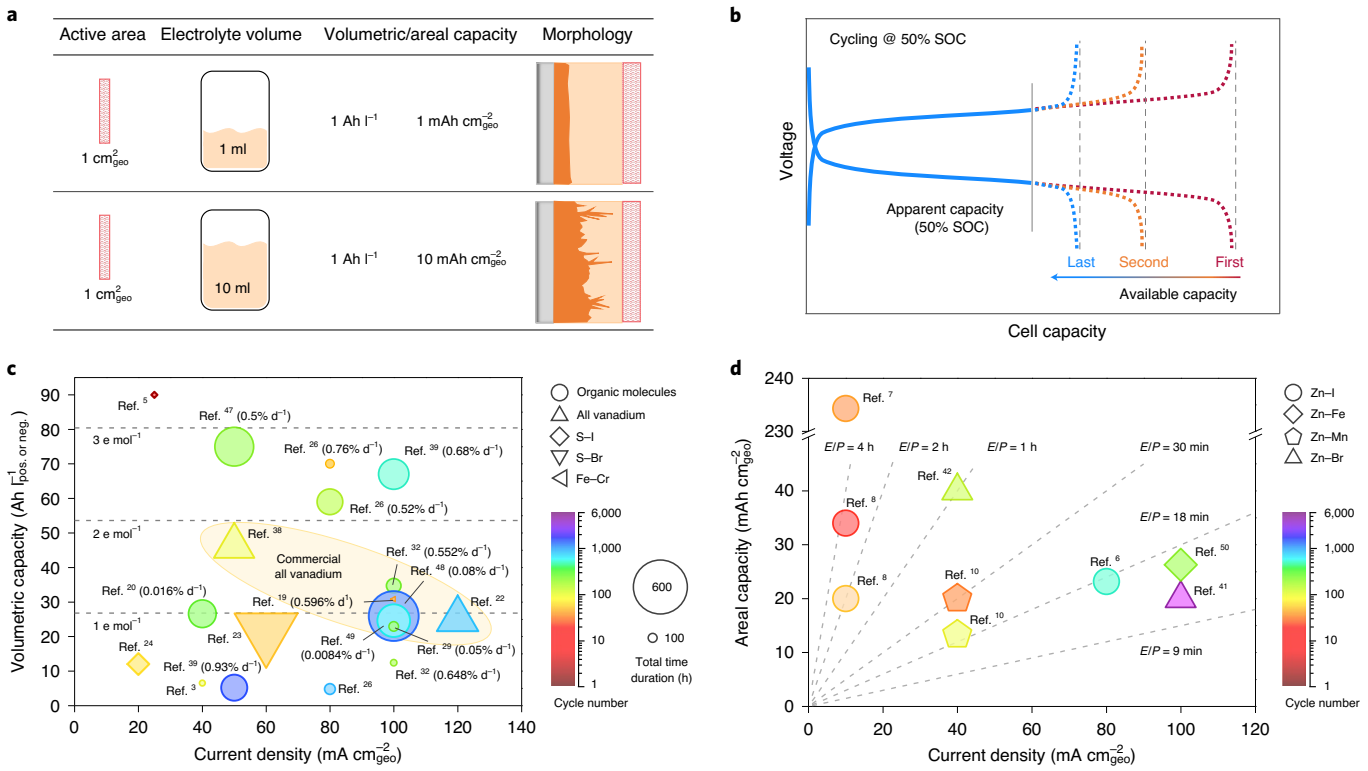

Fig. 2 | Role of areal capacity and SOC in RFB testing and summary of reported RFBs. a, Schematic of how electrolyte volume affects areal capacity. **b**, Schematic of hidden capacity fading due to low cycling SOC. The solid lines indicate the apparent capacity and the dashed lines indicate the available capacity. **c**,**d**, Summary of reported all-liquid (**c**) and solid-hybrid (**d**) RFBs at flow modes. All-liquid RFBs are analysed in four parameters: volumetric capacity (corresponding to electron concentration), current density, cycle number (heat map) and total time duration (symbol size)[3,5,19,20,22–24,26,29,32,38,39,47–49]. Solid-hybrid RFBs are analysed in three parameters: areal capacity, current density and cycle number (heat map)[6–8,10,41,42,50]. *E*/*P* (dashed line) represents the energy-to-power ratio, which is the discharge time duration of each cycle. See Source Data for details of each point.

could also cause capacity loss. These self-decomposition reactions may lead to permanent loss of active materials, low CE and capacity decay. For RFBs that are severely limited by self-decomposition, time-dependent capacity decay (% per day)[12,39] over a certain total period (day)[39] would be a critical assessment metric because self-decomposition is a time-sensitive process. Note that self-decomposition accelerates with the amount of active materials at play; therefore, both active material concentration and SOC should be considered when making these comparisons[35].

Electrolyte side reactions. Electrolyte side reactions such as solvent decompositions are common challenges facing RFBs. Water-splitting reactions including HER and OER are the main electrolyte side reactions in aqueous RFBs[40]. These side reactions are particularly problematic for active materials that operate beyond water-splitting potentials, leading to low CE, capacity imbalance and pH fluctuation, which could cause hydrolysis for transitional metal ions or OH^- nucleophilic attack for organic molecules[34]. As HER/OER are voltage-dependent decomposition processes, selecting suitable cycling voltage cut-off to minimize HER/OER is crucial to reveal the intrinsic stability of the RFBs. If the cut-off voltages overlap/exceed HER/OER potentials during cycling, both time-dependent and cycle-denominated metrics will reveal the capacity fade rate.

Dendrite formation and electrode passivation. Decay processes associated with uncontrolled solid deposition and incomplete dissolution are critical challenges for solid-hybrid RFBs. Metal dendrite formation (for example, zinc, lithium) consumes active materials and risks penetrating the membrane, leading to low CE, capacity decay and battery failure[41,42]. In addition to metal dendrites, redox couples involving the formation of a solid phase (for example, Mn^{2+}/MnO_2)[10] could also suffer from incomplete dissolution of solid products leading to electrode passivation, low CE and capacity decay. As dendrite formation and incomplete solid dissolution are strongly correlated to cycling areal capacity, flow rate and current density, these parameters are critical factors in assessing and comparing the stability of the solid-hybrid RFBs. Under comparable areal capacity and current density, cycle-denominated capacity decay rate would be a useful assessment metric for evaluating dendrite formation and electrode passivation as such decay accelerates with the frequency of deposition/dissolution.

Cell testing protocols and performance reporting practices

There are a large variety of RFB chemistries reported. It is therefore not our intention to cover specific testing details for all or any specific RFBs. Instead, we aim to discuss a general testing framework (and the rationales behind it) that can be principally applied to most RFB chemistries.

We consider three major RFB cell testing configurations, liquid-based symmetric cell, deposition-based symmetric cell and asymmetric full cell, under balanced or excess charge, static or flow modes. A symmetric cell employs the same active materials on both sides with different oxidation states and/or volumes to achieve balanced or excess charge[25,43]. Using excess charge for the counter electrolyte minimizes its negative impact on the cell capacity decay. Static cell refers to performing electrochemical cell measurements without circulating the electrolyte, which is suitable for initial materials screening but provides limited information on long-term

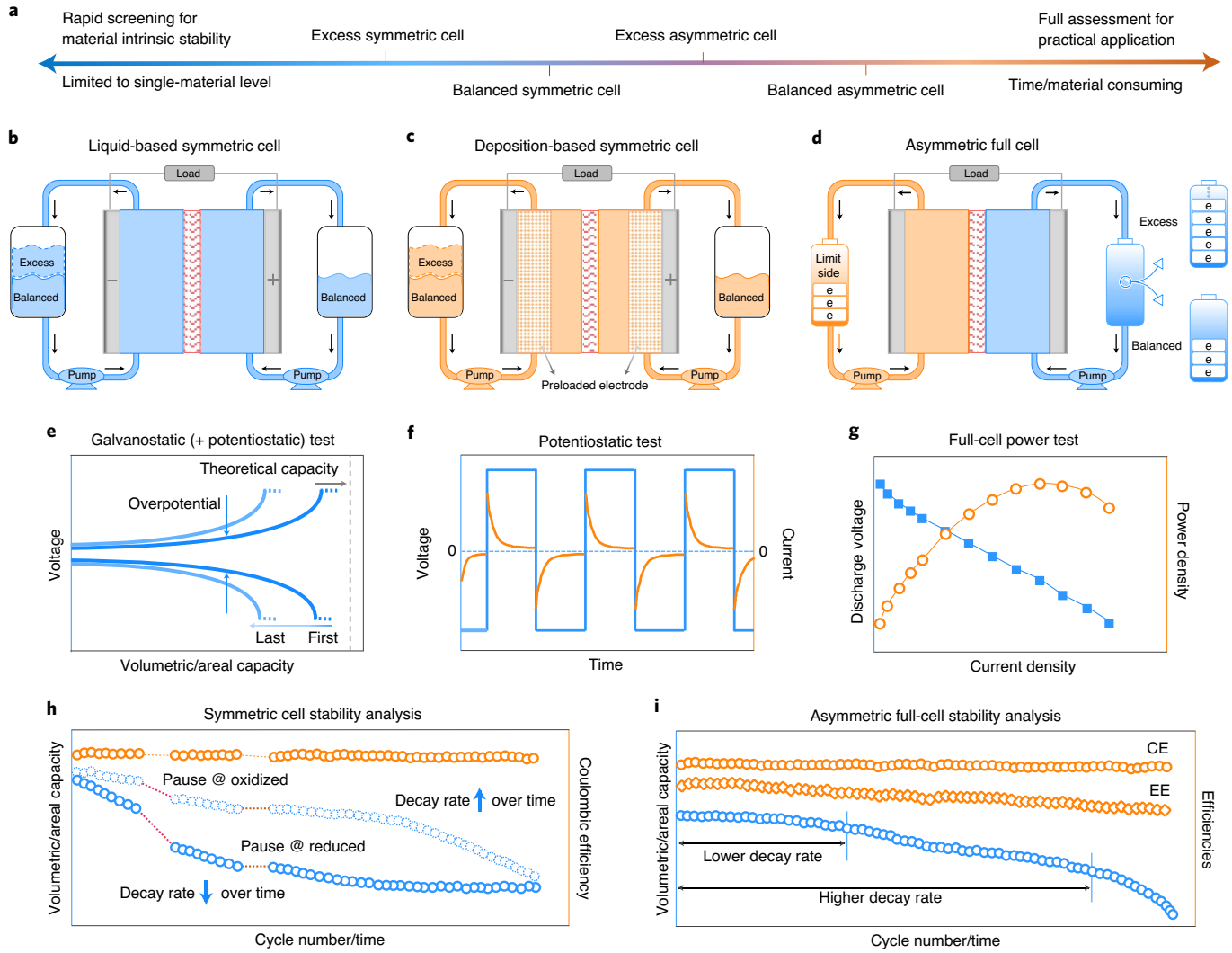

Fig. 3 | Recommended testing protocols and data analysis of three major RFB cell testing configurations. a, Pros and cons of different cell configurations. **b**–**d**, Testing protocols of liquid-based symmetric cell using 50% SOC electrolyte as the starting electrolyte (**b**), deposition-based symmetric cell using a pair of identical preloaded solid electrodes with an identical areal capacity (**c**) and asymmetric full cell using either excess counter electrolyte or balanced counter electrolyte (**d**). **e**,**f**, Schematic of voltage–current profile of three testing methods: galvanostatic test (or followed by a potentiostatic holding) (**e**) and potentiostatic holding (**f**). **g**, Power density measurement of asymmetric full cell at a selected SOC. **h**, Schematic of capacity-cycle/capacity-time analysis of symmetric cells along with CE. Time-dependent decay can be evaluated by pausing at the oxidized or reduced state. **i**, Schematic of capacity-cycle/capacity-time analysis of asymmetric cells along with CE and EE. The fluctuating nature of the decay rate requires comparisons to be conducted under a consistent time or cycle number.

practical applications. Operating flow cells requires proper designs of RFB cells (sealing, flow field, flow rate and so on) to eliminate gas/liquid leakage and optimize RFB performance. The flow field design is critical to achieve high power density and energy efficiency, especially for larger flow cells, which are often challenged by uneven distribution of electrolyte and high pump loss[44]. Effective flow field designs such as serpentine or interdigitated patterns have been shown to effectively reduce ohmic loss, enhance localized mass transfer in the electrode, and increase limiting current density and peak power density[44,45]. In addition, a flow rate design that minimizes the concentration overpotential and pump power consumption is critical in optimizing the overall system efficiency[44].

Performance metrics obtained from different test configurations/modes indicate different levels of maturity of the reported technology, from the single-material level to practical full-cell operation (Fig. 3a). Therefore, direct performance comparison across different configurations may give biased conclusions. While we focus on electrochemical assessment methods in this Perspective, we note that materials and mechanistic characterizations using spectroscopic and microscopic techniques are equally important to investigate the reaction and degradation mechanisms of RFBs[16].

Liquid-based symmetric cell. Liquid-based reactions refer to redox reactions that involve only soluble species. The excess symmetric cell configuration describes a charge-imbalanced cell with the same material on both sides having different oxidation states and/or volumes. The excess side has an excess charge to ensure the testing results are closely limited by the electrolyte of interest. As the amount of excess charge affects the overall capacity fade rate, it is recommended to identify the saturated excess charge beyond which point the capacity decay rate is no longer affected. This configuration probes the intrinsic stability of the material of interest free of irreversible chemical mixing from crossover. We note that extremely low crossover rate is a prerequisite for measuring capacity decay rate

in an excess symmetric cell to avoid diffusion of active materials from the excess electrolyte to the limited side. This concern can be addressed by using the balanced symmetric cell configuration in which both electrolytes exhibit the same amount of charge. In this case, the capacity decay is subject to intrinsic molecule decomposition, electrolyte side reactions (for example, HER/OER) and irreversible crossover at both sides. The symmetric cell measurements are suitable for initial material screening and stability evaluation at the single-material level, but it does not provide full assessments of how the material would perform at the full-cell level.

Recommended testing protocols and reporting metrics are summarized in Fig. 3b,e,f,h and Table 1. 50% SOC electrolyte should be used as the starting electrolyte by charging a cell from 0% SOC to 50% SOC in advance or simply mixing the electrolyte at 100% SOC and 0% SOC with the same volume (Fig. 3b). Two testing modes including potentiostatic (constant voltage, CV, Fig. 3f)[25] and galvanostatic–potentiostatic (constant current–constant voltage (CC–CV), Fig. 3e)[46] are recommended. The addition of a potential holding step after the CC process helps to fully utilize all the available active materials without influence from ohmic loss (for example, increase in membrane resistance). However, note that the CV method/step could promote side reactions (for example, OER/HER or solid iodine accumulation in iodide-based RFBs) and acquire extra capacity from the electrode capacitance effect. The former could be potentially mitigated by selecting holding potentials that are sufficiently far away from side reactions, although it is not straightforward when the potential of the target reaction is close to that of the unwanted reaction (for example I^-/I_3^- versus I^-/I_2). The latter could be in part calibrated by the pure capacitance measured from a cell without active species, and ensuring that the target redox capacity is orders of magnitude higher than the electrode capacitance to minimize its contribution.

As several RFB degradation processes accelerate with electrolyte concentration and SOC, performing symmetric cell measurements at a wide range of concentrations/SOCs provides a comprehensive understanding of RFB stabilities. However, high mass transport resistance associated with high electrolyte concentration could limit the achievable SOC even under the CV method[20]. This could be in part addressed by increasing the flow rate or increasing the holding overpotential, which, however, could increase electrolyte decomposition if the redox potential is close to the limits of the electrolyte stability window. During cycling, pausing under different SOCs helps to differentiate instability at the oxidized and reduced states[20]. As exemplified in Fig. 3h, the decay rate of the oxidized state is higher than the reduced state. In addition, as the capacity decay rate is normalized either by time or cycle numbers, it is important to report the total time duration and total cycle number along with the normalized values as the decay rate could change with time duration and cycle numbers, as illustrated by the different slopes of cycling stages in Fig. 3h,i.

Deposition-based symmetric cell. The deposition-based symmetric cell measures deposition/dissolution kinetics and reversibility of a redox reaction that involves solid phases. As dendrite formation and electrode passivation are their dominant decay mechanisms, areal capacity and current density are critical factors in assessments. A common way to study deposition reactions is to couple a metal foil with a deposition substrate using a symmetric electrolyte. However, it may not effectively reveal the intrinsic stability of the reaction in realistic applications considering that metal foil keeps compensating metal ions[13]. We recommend employing a symmetric cell using a pair of identical preloaded solid electrodes with an identical areal capacity to evaluate the solid-based reaction (Fig. 3c). The cycling areal capacity is set to fully dissolved and re-deposited on the electrode over the cycling measurement. This configuration accelerates all decay processes of solid deposition reactions including possible side reactions such as HER. The assessment method, reporting practice and performance metrics are similar to a liquid-based symmetric cell with additional emphasis on the areal capacity of the solid electrode (Fig. 3e,f,h and Table 1).

Asymmetric full cell. The excess asymmetric full-cell configuration describes a charge-imbalanced cell using two different materials in which one is the working electrolyte (limited charge) and the other serves as the counter electrolyte (excess charge) (Fig. 3d). This approach probes decays associated with the intrinsic stability (self-decomposition), irreversible crossover and electrolyte side reactions (OER/HER). Therefore, it is an important indicator to evaluate how the electrode/electrolyte would perform at the full-cell level. The purpose of employing excess charge in the counter electrolyte is to minimize its negative impact on the full-cell stability. The amount of excess charge can be categorized into low (≤1.5 times)[30,32], medium (1.5–3 times)[39] and high (≥3 times)[20]. While large excess charge minimizes the negative influence from the counter electrolyte, it sacrifices the overall energy density ($Wh\,l^{-1}_{pos.+neg.}$). Therefore, simultaneously achieving high energy density and high cycling stability is one of the most critical challenges for RFBs. If energy density is not of concern at a certain development stage, high excess charge (in both reduced and oxidized states) is recommended for assessing the stability of the capacity-limiting side. The balanced asymmetric full-cell configuration measures the electrochemical and chemical stability of both electrolytes in a charge-balanced cell (1:1)[33,38]. This approach assesses all performance metrics at the full-cell level that is the closest to the practical application. It is subject to all types of decay mechanisms. Therefore, the balanced asymmetric full cell is the harshest cell configuration.

Recommended testing protocols, data analysis and reporting metrics of asymmetric full cells are shown in Fig. 3e,g,i and Table 1. While excess charge can be achieved by different concentration and/or electrolyte volume, it is recommended to adjust the electrolyte volume while keeping a similar concentration at both sides to avoid creating a large concentration difference and water migration from osmotic pressure. Power density measurement can be performed by discharging the cell at various SOCs and current densities (Fig. 3g). For a long-term stability test, while cycling at 100% SOC comprehensively evaluates capacity decay, it is not commonly used in commercial RFBs. Alternatively, performing 100% SOC only at a certain frequency[46] or conducting concentration analysis (titration, ultraviolet–visible and so on) before and after cycling at practical SOCs could be used to evaluate the cycling stability of the RFB.

For all cell configurations, several important testing parameters should be reported together with performance metrics. This includes SOC, current density/voltage amplitude, cut-off voltage/current/capacity, electrolyte concentration, electrolyte volume, thickness and area of membrane and electrode, designs of flow field, testing environment in the ambient air or an inert glovebox, testing temperature and flow rate.

Conclusions

In this Perspective, we discuss assessment methods, performance metrics, degradation mechanisms and common misconceptions in RFBs. We generalize RFBs into all-liquid and solid-hybrid RFBs with four major degradation mechanisms (crossover, self-decomposition of active materials, electrolyte side reaction, and dendrite formation and electrode passivation). We discuss assessment metrics in direct relation to the limiting processes of RFBs. Common misconceptions in calculating volumetric capacity/energy, interpreting areal capacity in solid electrodes, and understanding and applying SOC and CE in long-term stability tests are discussed. Finally, we discuss general testing framework, data analysis and reporting practices to facilitate future RFB benchmarking and development.

Received: 14 September 2020; Accepted: 17 December 2020;
Published online: 11 February 2021

References

1. Park, M., Ryu, J., Wang, W. & Cho, J. Material design and engineering of next-generation flow-battery technologies. *Nat. Rev. Mater.* **2**, 16080 (2016).
2. Li, L. et al. A stable vanadium redox-flow battery with high energy density for large-scale energy storage. *Adv. Energy Mater.* **1**, 394–400 (2011).
3. Janoschka, T. et al. An aqueous, polymer-based redox-flow battery using non-corrosive, safe, and low-cost materials. *Nature* **527**, 78–81 (2015).
4. Huskinson, B. et al. A metal-free organic–inorganic aqueous flow battery. *Nature* **505**, 195–198 (2014).
5. Li, Z., Weng, G., Zou, Q., Cong, G. & Lu, Y.-C. A high-energy and low-cost polysulfide/iodide redox flow battery. *Nano Energy* **30**, 283–292 (2016).
6. Xie, C., Liu, Y., Lu, W., Zhang, H. & Li, X. Highly stable zinc-iodine single flow batteries with super high energy density for stationary energy storage. *Energy Environ. Sci.* **12**, 1834–1839 (2019).
7. Li, B. et al. Ambipolar zinc-polyiodide electrolyte for a high-energy density aqueous redox flow battery. *Nat. Commun.* **6**, 6303 (2015).
8. Weng, G.-M., Li, Z., Cong, G., Zhou, Y. & Lu, Y.-C. Unlocking the capacity of iodide for high-energy-density zinc/polyiodide and lithium/polyiodide redox flow batteries. *Energy Environ. Sci.* **10**, 735–741 (2017).
9. Zhao, Y. et al. A chemistry and material perspective on lithium redox flow batteries towards high-density electrical energy storage. *Chem. Soc. Rev.* **44**, 7968–7996 (2015).
10. Xie, C. et al. A highly reversible neutral zinc/manganese battery for stationary energy storage. *Energy Environ. Sci.* **13**, 135–143 (2020).
11. Wang, Z., Tam, L.-Y. S. & Lu, Y.-C. Flexible solid flow electrodes for high-energy scalable energy storage. *Joule* **3**, 1677–1688 (2019).
12. Kwabi, D. G., Ji, Y. & Aziz, M. J. Electrolyte lifetime in aqueous organic redox flow batteries: a critical review. *Chem. Rev.* **120**, 6467–6489 (2020).
13. Xiao, J. et al. Understanding and applying Coulombic efficiency in lithium metal batteries. *Nat. Energy* **5**, 561–568 (2020).
14. Darling, R., Gallagher, K., Xie, W., Su, L. & Brushett, F. Transport property requirements for flow battery separators. *J. Electrochem. Soc.* **163**, A5029–A5040 (2015).
15. Chen, Q., Eisenach, L. & Aziz, M. J. Cycling analysis of a quinone-bromide redox flow battery. *J. Electrochem. Soc.* **163**, A5057–A5063 (2016).
16. Tong, L. et al. UV-vis spectrophotometry of quinone flow battery electrolyte for in situ monitoring and improved electrochemical modeling of potential and quinhydrone formation. *Phys. Chem. Chem. Phys.* **19**, 31684–31691 (2017).
17. Skyllas-Kazacos, M., Kazacos, G., Poon, G. & Verseema, H. Recent advances with UNSW vanadium-based redox flow batteries. *Int. J. Energy Res.* **34**, 182–189 (2010).
18. Perry, M. L., Saraidaridis, J. D. & Darling, R. M. Crossover mitigation strategies for redox-flow batteries. *Curr. Opin. Electrochem.* **21**, 311–318 (2020).
19. Waters, S. E., Robb, B. H. & Marshak, M. P. Effect of chelation on iron-chromium redox flow batteries. *ACS Energy Lett.* **5**, 1758–1762 (2020).
20. Jin, S. et al. Near neutral pH redox flow battery with low permeability and long-lifetime phosphonated viologen active species. *Adv. Energy Mater.* **10**, 2000100 (2020).
21. Dong, Y.-R., Kaku, H., Hanafusa, K., Moriuchi, K. & Shigematsu, T. A novel titanium/manganese redox flow battery. *ECS Trans.* **69**, 59–67 (2015).
22. Yuan, Z. et al. Advanced porous membranes with ultra-high selectivity and stability for vanadium flow batteries. *Energy Environ. Sci.* **9**, 441–447 (2016).
23. Zhou, H., Zhang, H., Zhao, P. & Yi, B. A comparative study of carbon felt and activated carbon based electrodes for sodium polysulfide/bromine redox flow battery. *Electrochim. Acta* **51**, 6304–6312 (2006).
24. Ma, D. et al. Highly active nanostructured CoS_2/CoS heterojunction electrocatalysts for aqueous polysulfide/iodide redox flow batteries. *Nat. Commun.* **10**, 3367 (2019).
25. Goulet, M.-A. & Aziz, M. J. Flow battery molecular reactant stability determined by symmetric cell cycling methods. *J. Electrochem. Soc.* **165**, A1466–A1477 (2018).
26. Zhang, C. et al. Phenothiazine-based organic catholyte for high-capacity and long-life aqueous redox flow batteries. *Adv. Mater.* **31**, 1901052 (2019).
27. Park, M. et al. A high voltage aqueous zinc–organic hybrid flow battery. *Adv. Energy Mater.* **9**, 1900694 (2019).
28. Beh, E. S. et al. A neutral pH aqueous organic–organometallic redox flow battery with extremely high capacity retention. *ACS Energy Lett.* **2**, 639–644 (2017).
29. Kwabi, D. G. et al. Alkaline quinone flow battery with long lifetime at pH 12. *Joule* **2**, 1894–1906 (2018).
30. Lin, K. et al. A redox-flow battery with an alloxazine-based organic electrolyte. *Nat. Energy* **1**, 16102 (2016).
31. Liu, T., Wei, X., Nie, Z., Sprenkle, V. & Wang, W. A total organic aqueous redox flow battery employing a low cost and sustainable methyl viologen anolyte and 4-HO-TEMPO catholyte. *Adv. Energy Mater.* **6**, 1501449 (2016).
32. Liu, Y. et al. A long-lifetime all-organic aqueous flow battery utilizing TMAP-TEMPO radical. *Chem* **5**, 1861–1870 (2019).
33. Hu, B., DeBruler, C., Rhodes, Z. & Liu, T. L. Long-cycling aqueous organic redox flow battery (AORFB) toward sustainable and safe energy storage. *J. Am. Chem. Soc.* **139**, 1207–1214 (2017).
34. Yang, B. et al. High-performance aqueous organic flow battery with quinone-based redox couples at both electrodes. *J. Electrochem. Soc.* **163**, A1442–A1449 (2016).
35. Goulet, M.-A. et al. Extending the lifetime of organic flow batteries via redox state management. *J. Am. Chem. Soc.* **141**, 8014–8019 (2019).
36. Tong, L. et al. Molecular engineering of an alkaline naphthoquinone flow battery. *ACS Energy Lett.* **4**, 1880–1887 (2019).
37. Xie, C., Duan, Y., Xu, W., Zhang, H. & Li, X. A low-cost neutral zinc-iron flow battery with high energy density for stationary energy storage. *Angew. Chem. Int. Ed.* **56**, 14953–14957 (2017).
38. Roe, S., Menictas, C. & Skyllas-Kazacos, M. A high energy density vanadium redox flow battery with 3 M vanadium electrolyte. *J. Electrochem. Soc.* **163**, A5023–A5028 (2015).
39. Hollas, A. et al. A biomimetic high-capacity phenazine-based anolyte for aqueous organic redox flow batteries. *Nat. Energy* **3**, 508–514 (2018).
40. Li, Z. & Lu, Y.-C. Material design of aqueous redox flow batteries: fundamental challenges and mitigation strategies. *Adv. Mater.* **32**, 2002132 (2020).
41. Lee, J.-H. et al. Dendrite-free Zn electrodeposition triggered by interatomic orbital hybridization of Zn and single vacancy carbon defects for aqueous Zn-based flow batteries. *Energy Environ. Sci.* **13**, 2839–2848 (2020).
42. Yin, Y. et al. Dendrite-free zinc deposition induced by tin-modified multifunctional 3D host for stable zinc-based flow battery. *Adv. Mater.* **32**, 1906803 (2020).
43. Darling, R. M. & Perry, M. L. Half-cell, steady-state flow-battery experiments. *ECS Trans.* **53**, 31–38 (2013).
44. Ke, X. et al. Rechargeable redox flow batteries: flow fields, stacks and design considerations. *Chem. Soc. Rev.* **47**, 8721–8743 (2018).
45. Zheng, Q., Xing, F., Li, X., Ning, G. & Zhang, H. Flow field design and optimization based on the mass transport polarization regulation in a flow-through type vanadium flow battery. *J. Power Sources* **324**, 402–411 (2016).
46. Brushett, F. R., Aziz, M. J. & Rodby, K. E. On lifetime and cost of redox-active organics for aqueous flow batteries. *ACS Energy Lett.* **5**, 879–884 (2020).
47. Jin, S. et al. A water-miscible quinone flow battery with high volumetric capacity and energy density. *ACS Energy Lett.* **4**, 1342–1348 (2019).
48. Wang, C. et al. Molecular design of fused-ring phenazine derivatives for long-cycling alkaline redox flow batteries. *ACS Energy Lett.* **5**, 411–417 (2020).
49. Wu, M. et al. Extremely stable anthraquinone negolytes synthesized from common precursors. *Chem* **6**, 1432–1442 (2020).
50. Yuan, Z., Duan, Y., Liu, T., Zhang, H. & Li, X. Toward a low-cost alkaline zinc-iron flow battery with a polybenzimidazole custom membrane for stationary energy storage. *iScience* **3**, 40–49 (2018).

Acknowledgements

The work described herein was supported by a grant from the Research Grant Council (RGC) of the Hong Kong Special Administrative Region, China (project number T23-601/17-R).

Competing interests

The authors declare no competing interests.

Additional information

Supplementary information The online version contains supplementary material available at https://doi.org/10.1038/s41560-020-00772-8.

Correspondence should be addressed to Y.-C.L.

Peer review information *Nature Energy* thanks Travis Anderson, Mike Perry and Wei Wang for their contribution to the peer review of this work.

Reprints and permissions information is available at www.nature.com/reprints.

Publisher's note Springer Nature remains neutral with regard to jurisdictional claims in published maps and institutional affiliations.